Chemistry–A European Journal
Research Article
doi.org/10.1002/chem.202300196
Chemistry Europe
European Chemical Societies Publishing

www.chemeurj.org

Boronic Acid Assisted Self-Assembly of Functional RNAs

Amandine Lelièvre-Büttner,[a] Theodor Schnarr,[a] Mégane Debiais,[b] Michael Smietana,*[b] and Sabine Müller*[a]

Abstract: Boronate esters formed by reaction of an oligonucleotide carrying a 5′-boronic acid moiety with the 3′-terminal *cis*-diol of another have been shown previously to assist assembly of fragmented DNAzymes. Here we demonstrate that boronate esters replacing the natural phosphodiester linkage at selected sites of two functional RNAs, the hairpin ribozyme and the Mango aptamer, allow assembly of functional structures. The hairpin ribozyme, a small naturally occurring RNA that supports the reversible cleavage of appropriate RNA substrates, is very sensitive to fragmentation. Splitting the ribozyme at four different sites led to a significant decrease or even loss of cleavage and ligation activity. Ribozymes assembled from fragments capable of boronate ester formation showed restoration of cleavage activity in some but not all cases, dependent on the split site. Ligation proved to be more challenging, no supportive effect of the boronate ester was observed. Split variants of the Mango aptamer also showed a dramatic loss of functionality, which however, was restored when 5′-boronic acid modified fragments were used for assembly. These studies show for the first time that boronate esters as internucleoside linkages can act as surrogates of natural phosphodiesters in functional RNA molecules.

Introduction

Understanding the origin of life and developing models and hypotheses for experimental proof is a field of research that is as fascinating as it is challenging. In studies underpinning the RNA world hypothesis, the emergence of first RNA strands and moreover of first functional RNAs has been a long-standing question. Much effort has been made in developing scenarios of arbitrary RNA polymerization from monomers[1] as well as in finding RNA enzymes that catalyze the replication of RNA molecules, including the enzyme itself.[2] Alternatively, first oligonucleotides could have been assembled from activated short oligomers[3] or by formation of dynamic internucleosidic linkages[4,5] in enzyme-free conditions, providing the capacity of self-healing, -replicating or -adapting.[6,7]

Apart from the RNA world scenario, RNA self-assembly from shorter fragments is an issue of interest in the field of diagnostics. Previously, we have reviewed the area of split aptamers and nucleic acid enzymes for the development of advanced biosensors.[8] The concept of split aptamers relies on dissecting an aptamer in two or more fragments with the capability of assembling in the presence of the cognate target. In order to enhance stability, individual fragments can be decorated with functionalities that allow covalent end-joining of the fragments upon assembling. Also here, dynamic internucleosidic linkages are of interest, because they allow reversibility and control of functionality.[9,10] In this context, the spontaneous and reversible reaction of boronic acid with a *cis*-diol, yielding a cyclic boronate ester is a suitable chemistry for the formation of dynamic internucleosidic linkages. Boronic acids are sufficiently stable to operate in aqueous media, and thus we have previously demonstrated reversible DNA- and RNA-templated boronate ester formation by using one set of fragments carrying a boronic acid group at the 5′-terminus and another set of fragments terminated with a ribonucleotide to provide the *cis*-diol required for boronate ester formation (Figure 1A).[11–14] So far, we concentrated on the synthesis of 5′-boronic acid modified deoxynucleotides and boronate ester formation between DNA fragments having the required 5′- and 3′-functionalities. Nevertheless, we have also started to synthesize 5′-boronic acid modified ribonucleotides and accordingly 5′-boronic acid functionalized RNA strands. Using these strands for duplex formation with an opposite RNA strand as depicted in Figure 1B, we observed the formation of RNA hairpin loops by reaction of a 5′-terminal boronic acid group of the short RNA strand with the *cis*-diol terminating the 3′-overhang of the longer RNA strand.[12]

More recently, we have used this chemistry for the study of split DNAzymes.[15] The 10–23 DNAzyme, one of the first and most widely studied DNAzymes,[16] was used as the parent structure, from which several split versions with restored activity were derived from 5′-boronic acid and cis-diol- containing fragments.[15]

[a] *Dr. A. Lelièvre-Büttner, T. Schnarr, Prof. Dr. S. Müller*
Institute of Biochemistry
University of Greifswald
Felix-Hausdorff-Straße 4, 17489 Greifswald (Germany)
E-mail: sabine.mueller@uni-greifswald.de

[b] *Dr. M. Debiais, Prof. Dr. M. Smietana*
Institut des Biomolécules Max Mousseron
Université de Montpellier, CNRS, ENSCM
1919 route de Mende 34293 Montpellier (France)
E-mail: michael.smietana@umontpellier.fr

Supporting information for this article is available on the WWW under https://doi.org/10.1002/chem.202300196

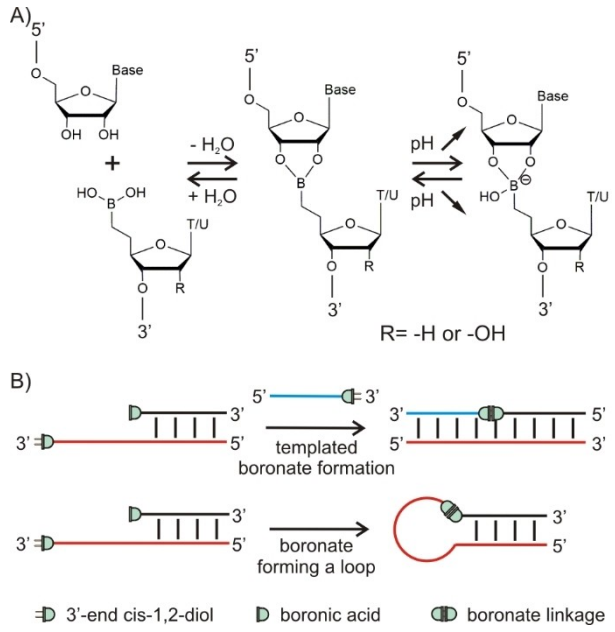

Figure 1. A) Formation of an internucleosidic boronate ester linkage. **B)** Schematic representation of boronic acid-assisted formation of a RNA duplex and a RNA hairpin as reported in Ref. [12].

Here, we set out to explore the activity of split versions of the light-up aptamer Mango[17] and of the hairpin ribozyme using the boronate chemistry described above for assistance of fragment assembly. In contrast to the rather small and robust 10–23 DNAzyme, the hairpin ribozyme being a more complex RNA catalyst was expected to be more sensitive towards fragment splitting. Apart from the comparison with the split DNAzyme, demonstration of the ability of RNA pieces to assemble and form a functional RNA catalyst, would be not only a promising concept for biosensing or therapeutic application, but provide an appealing model for the generation of functional RNAs assembled from smaller non-functional fragments in early life.

The hairpin ribozyme is a small naturally occurring RNA motif derived from the tobacco ringspot virus satellite RNA ((−)sTRSV).[18] The minimal structure consists of four helices interrupted by two loops (A and B), and it catalyzes the reversible cleavage of a specific phosphodiester bond in the presence of Mg^{2+} (Figure 2).[19,20] Numerous hairpin ribozyme variants have been designed in the past for structural studies as well as for specific applications.[21–24] However, compared to the number of split DNA/RNA aptamer systems reviewed recently,[8] reports on fragmented ribozymes are scarce. In many studies, three-stranded hairpin ribozyme versions have been used for the reason of more efficient chemical synthesis of shorter RNA strands, rather than for the purpose of studying the effect of fragmentation on activity as such.[25,26] In the present work, we engineered new split-hairpin ribozyme variants and studied their cleavage and ligation activity. In particular, we looked at the performance of 5′-boronic acid modified fragments in the

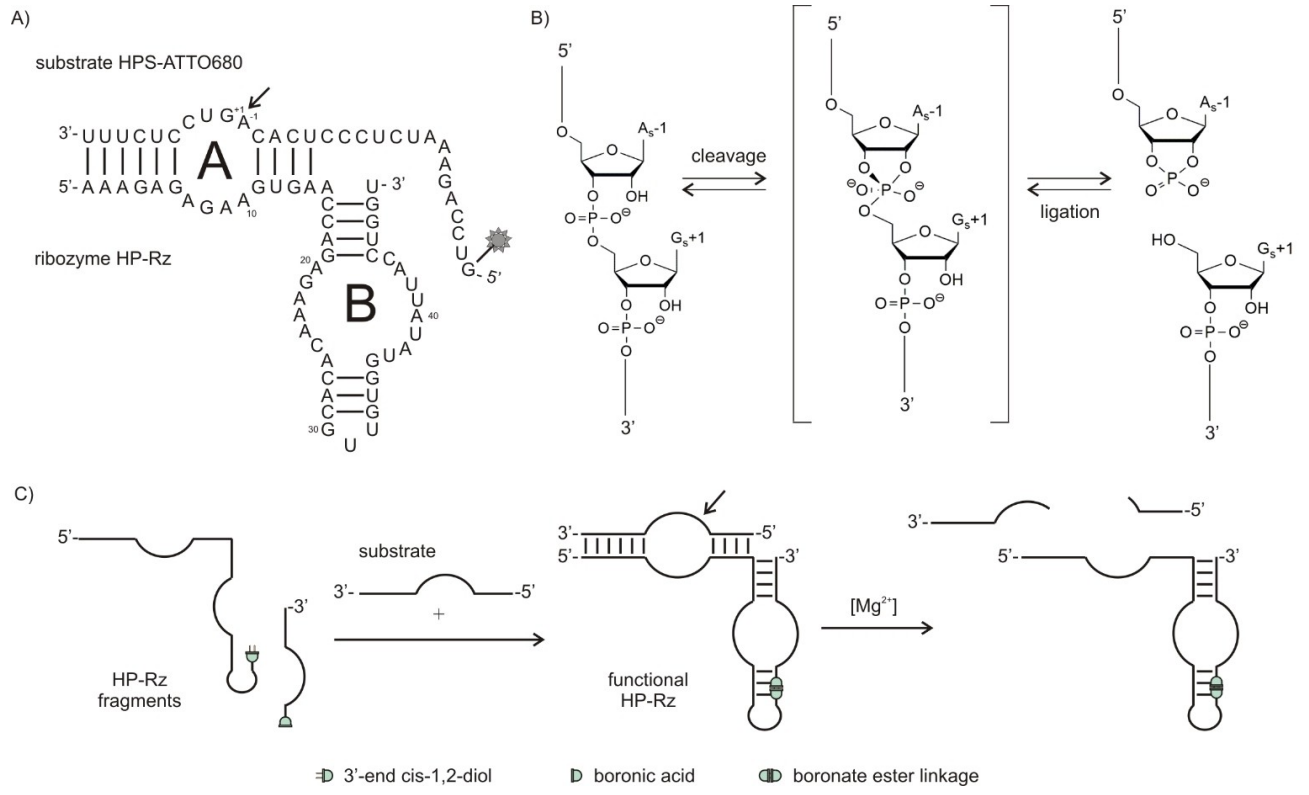

Figure 2. A) Secondary structure of the hairpin ribozyme bound to the ATTO680 labelled substrate. **B)** Mechanism of reversible RNA cleavage by the hairpin ribozyme.[28] **C)** Schematic representation of the boronic acid-assisted assembly of a split-hairpin ribozyme to form a functional structure.

split variants in comparison to their unmodified counterparts (Figure 2C). As described above, the boronate ester linkage, if formed, would stabilize the assembled ribozyme, and this should mirror in higher activity as compared to the respective non-modified split variant. In addition to the hairpin ribozyme, we also studied the assembly and restoration of functionality by boronic acid ester formation in a split version of the light-up RNA aptamer Mango to improve the design and performance of split light up aptameric sensors for intracellular monitoring and imaging of biomolecules.[27]

Results

Design of the split ribozyme variants

Four different split hairpin ribozyme variants were designed and investigated. For this purpose, the hairpin ribozyme was split in two fragments individually at the sites depicted in Figure 3A. To follow activity, the RNA substrates to be cleaved or ligated were fluorescently labelled with ATTO680, and the reaction rate constants were determined by quantification of the amount of cleaved or ligated RNA over time after separation by gel electrophoresis. Since originally the dynamic internucleosidic boronate ester backbone was shown to be more stable in templated conditions,[11] we first investigated split-hairpin ribozyme variants that were fragmented in the stem areas (Figure 3A). Variants with different split sites were named in

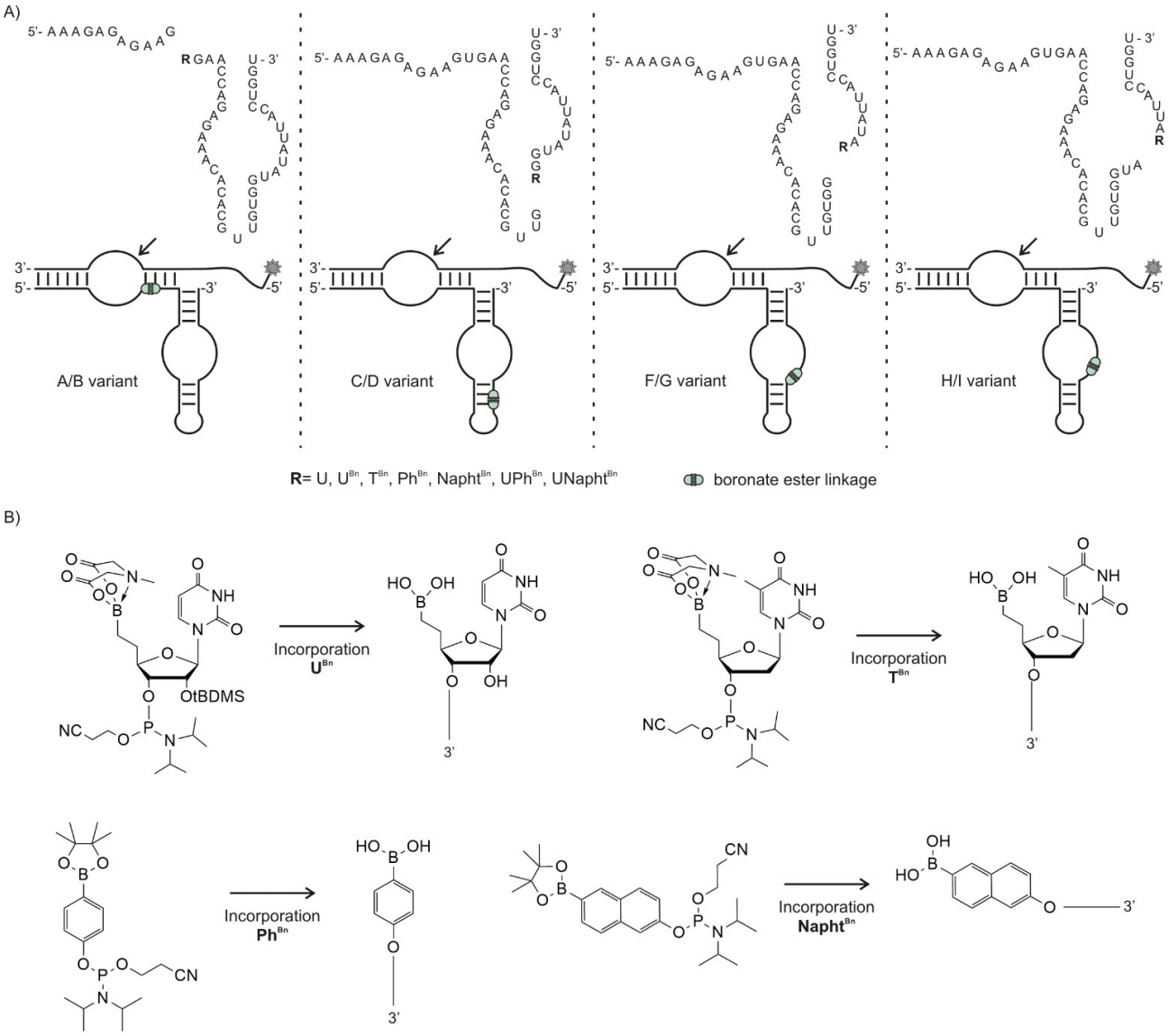

Figure 3. A) Sequences of the hairpin ribozyme fragments and secondary structures showing the site of the boronate ester linkage. **B)** Phosphoramidite building blocks of boronic acid derivatives used in the study and obtained RNAs with 3′-terminal boronic acid moieties.

alphabetical order according to the fragments they are assembled from. Variant **A/B** was split between G^{11} and U^{12}, and variant **C/D** between G^{33} and U^{34}. Furthermore, based on our previous studies on DNAzymes with the split site in the catalytic loop[15] and on boronic acid ester assisted RNA loop formation,[12] we included two more split hairpin ribozyme variants in our study: variant **F/G** with the split site between G^{36} and U^{37}, and variant **H/I** with the split site between A^{38} and U^{39} in loop B (Figure 3A). The two uridines U^{37} and U^{39} are known not to be involved in essential tertiary interactions,[29] making them suitable sites for modification with the 5′-borono derivatives.

Preparation of split ribozyme variants and substrate RNA

All required RNA fragments **A** to **I** were prepared by solid-phase chemical synthesis. For fragments **B**, **D**, **G**, and **I**, 5′-boronic acid modified versions were synthesized in addition to the non-modified strands. Commercially available 4-hydrophenylboronic acid (**Ph^{Bn}**) and 6-hydroxyl-2-naphtaleneboronic acid (**Napht^{Bn}**), as well as previously synthesized 5′-boronothymidine (**T^{Bn}**) and 5′-boronouridine (**U^{Bn}**)[12,30] were converted to the corresponding phosphoramidites and coupled as last building block to the 5′-end of fragments **B**, **D**, **G**, and **I** (Figure 3B). The modified strands were named according to the type of modification: **X^{TBn}** for strands carrying **T^{Bn}** at their 5′-end, and **X^{UBn}** for strands modified with **U^{Bn}**. In case of modification with **Ph^{Bn}** and **Napht^{Bn}**, two strands were synthesized; one strand where the modification was added to the 5′-end (named **X^{UPhBn}** or **X^{UNaphtBn}**) and one strand where the last 5′-end uridine was replaced with the modification (named **X^{PhBn}** or **X^{NaphtBn}**). The full-length hairpin ribozyme **HP-Rz**, used as control, was prepared by in-vitro transcription. In order to allow the cleavage reaction to be followed, the substrate strand HPS was chemically synthesized and functionalized with a 5′-terminal amine, to which ATTO680-NHS ester was coupled post-synthetically.

Cleavage reactions

The cleavage activity was first evaluated for the parent ribozyme **HP-Rz** in the presence of 20 mM $MgCl_2$ at 25 °C and pH 7.5, and at saturating ribozyme concentration (Table 1, Figure S17). The cleavage rate ($k_{obs} = 0.105 \pm 0.015$ min^{-1}) is somewhat lower as usually observed for the hairpin ribozyme, which is a consequence of the lower temperature (25 °C instead of 37 °C). The temperature of 25 °C for the cleavage reaction was chosen with regard to the split HP-Rz variants, which would be less stable at the standard temperature of 37 °C. We then looked at the unmodified split ribozymes, where only **HP-Rz C/D** showed activity, although significantly lower than observed for the parent **HP-Rz** (k_{obs} **C/D** $= 0.012 \pm 0.001$ min^{-1}). None of the other unmodified split versions showed significant cleavage activity within 3 h, such that rate constants could not be measured (Table S5).

Next, we evaluated the cleavage activity of split HP-Rz variants using fragments carrying at their 5′-end the borono modifications mentioned above and shown in Table 1. Individual variants of split ribozyme **HP-Rz C/D** were assembled from unmodified fragment **C** and fragment **D**, 5′-functionalized with either of the boronic acid moieties shown in Figure 3B. The time courses of cleavage reactions are summarized in Figure S9. Kinetic graphs for all **C/D** variants are shown in Figures S10 to S17 and corresponding data presented in Table 1. Recovery of cleavage activity was observed in particular with fragment **D** carrying a 5′-terminal borono-uridine (**D^{UBn}**) and to somewhat lesser extent but still significant with fragment **D** carrying a 5′-terminal borono-thymidine (**D^{TBn}**). Cleavage rate constants increased by a factor of 1,5 to 2, and cleavage efficiency was restored from 32 % (unmodified split variant **C/D**) to 54.0 % and 45 % for the two borono-modified variants **C/D^{UBn}** and **C/D^{TBn}**, (Table 1, Table S5).

When adding the non-nucleosidic borono moieties **Ph^{Bn}** and **Napht^{Bn}** to the 5′-end of fragment **D**, cleavage activity remained the same or was even worse than that observed for the unmodified split ribozyme variant **C/D** (Figure 2C, Table 1, Figure S9, Table S5). Here, certainly destabilization of helix 4 by the additional phenylboronic acid or naphtylboronic acid moiety plays a role and can explain at least in part the observed result. It remains questionable, if the boronate ester has formed at all, since the structure at the templated ligation site clearly must be distorted. Thus with both variants, **C/D^{UPhBn}** and **C/D^{UNaphtBn}**, cleavage reached only 31 to 34 % (Table 1). When the entire 5′-terminal uridine (U^{34}) of fragment **D** was replaced with either Phenylboronic acid or Naphtylboronic acid, activity was

Table 1. Cleavage efficiency (a, %) and observed cleavage rate constant (k_{obs}, min^{-1}) of split ribozyme variants at 25 °C, 20 mM $MgCl_2$, pH 7.5 and 8.7.

Entry	Variants	% cleav. pH 7.5	% cleav. pH 8.7	k_{obs} pH 7.5	k_{obs} pH.8.7
1	HP-Rz	56.76 ± 2.46	69.32 ± 2.35	0.105 ± 0.015	0.111 ± 0.024
2	HP-Rz **C/D**	32.13 ± 1.31	39.88 ± 1.84	0.012 ± 0.001	0.014 ± 0.002
3	HP-Rz **C/D^{UBn}**	54.45 ± 1.59	62.03 ± 1.55	0.018 ± 0.001	0.033 ± 0.002
4	HP-Rz **C/D^{TBn}**	45.27 ± 1.87	60.66 ± 1.27	0.021 ± 0.002	0.035 ± 0.002
5	HP-Rz **C/D^{UPhBn}**	31.19 ± 3.89	44.06 ± 1.72	0.013 ± 0.003	0.010 ± 0.001
6	HP-Rz **C/D^{PhBn}**	28.36 ± 1.87	30.27 ± 1.31	0.007 ± 0.001	0.010 ± 0.001
7	HP-Rz **C/D^{UNaphtBn}**	34.24 ± 1.18	29.71 ± 1.28	0.005 ± 0.0002	0.008 ± 0.0006
8	HP-Rz **C/D^{NaphtBn}**	26.58 ± 1.34	32.84 ± 0.46	0.016 ± 0.002	0.014 ± 0.0004

Note: values were obtained from nonlinear exponential fitting of data sets collected from the cleavage reaction, using the equation $y = a(1-e^{-bx})$ (a and b represent the final cleavage efficiency and the observed rate of the reaction, respectively) using Origin 8.

even worse. Both split ribozyme variants **C/D^{PhBn}** and **C/D^{NaphtBn}** reached only 28% and 27% cleavage, which is most likely a consequence of the missing A38:U34 base pair in helix 4. Again, the formation of the boronate ester remains questionable in these cases, due to the distance between the 5′-terminal boronic acid of one fragment and the 3′-terminal *cis*-diol of the other, when bound to the complementary sequence forming helix 4.

Boronate ester formation is supported under basic conditions, assisting rehybridisation of the sp^2 boron to a tetrahedral sp^3 anion.[31] Therefore, we have conducted cleavage experiments with all **C/D** variants at higher pH (Table 1, Figure S9, Table S5). When looking at the percentage of cleavage, it is increased in all cases, although the increase is most pronounced for **C/D^{UBn}** and **C/D^{TBn}**. The full length ribozyme **HP-Rz** also shows a higher cleavage yield at pH 8.7. Thus, the increase cannot necessarily be interpreted as a consequence of better stabilization of the formed boronate ester, but may be as well a consequence of the better activation of the attacking nucleophile at higher pH. Regarding cleavage kinetics however, an effect was clearly observed for split variants **C/D^{UBn}** and **C/D^{TBn}**, where cleavage rates increased about two-fold when changing pH from 7.5 to 8.7 (Table 1). All other variants did not show significant changes in the reaction rate. This speaks for the expected stabilization of the boronate ester at higher pH, if properly positioned in the ribozyme structure, and in consequence for improved stability of the folded ribozyme mirrored in higher observed cleavage rates k_{obs}. Encouraged by these results, we decided to study other split regions and designed further split ribozyme variants (**A/B**, **F/G** and **H/I**) (Figure 4). In the **A/B** variant, the split site is positioned within helix 2 between G^{11} and U^{12} (for nucleotide numbering compare Figure 2A). The position was chosen due to the fact that only the 5′-borono derivative of uridine was available for incorporation into RNA, hence we looked for 5′N*U-3′ sites (the asterisk marks the split position) and defined $G^{11}U^{12}$ as a possible site. In addition to templated split sites within helices, we also sought to investigate if we can split the ribozyme within loop B, and defined $G^{36}U^{37}$ and $A^{38}U^{39}$ as two more possible split sites to constitute split ribozyme variants **F/G** and **H/I**.

All three split variants showed significantly reduced activity in comparison to the parent full-length ribozyme (Figure 4, Table S5). The same cleavage conditions as for the **C/D** variants were used, but the reaction time was extended to 144 h, since virtually no cleavage was observed within the previously used three hours. Cleavage activity of split variant **A/B** was very poor (1.5% after 144 h) but could be somewhat improved (6.5% after 144 h) when the 5′-boronouridine carrying fragment was present (**A/B^{UBn}**, Figure 4A, Table S5). To our surprise, also variants **F/G** and **H/I** with the split site located in a loop region, showed unexpected activity (39±2% and 17±1% after 144 h), even higher than the **A/B** variant with the templated split site in helix 2 (Figure 4B and C, Table S5). When a boronate ester was formed with the 5′-U^{Bn} carrying fragment, cleavage activity of the corresponding variant **F/G^{UBn}** was clearly improved, reaching about 50% conversion after 144 h. Fragment **G**

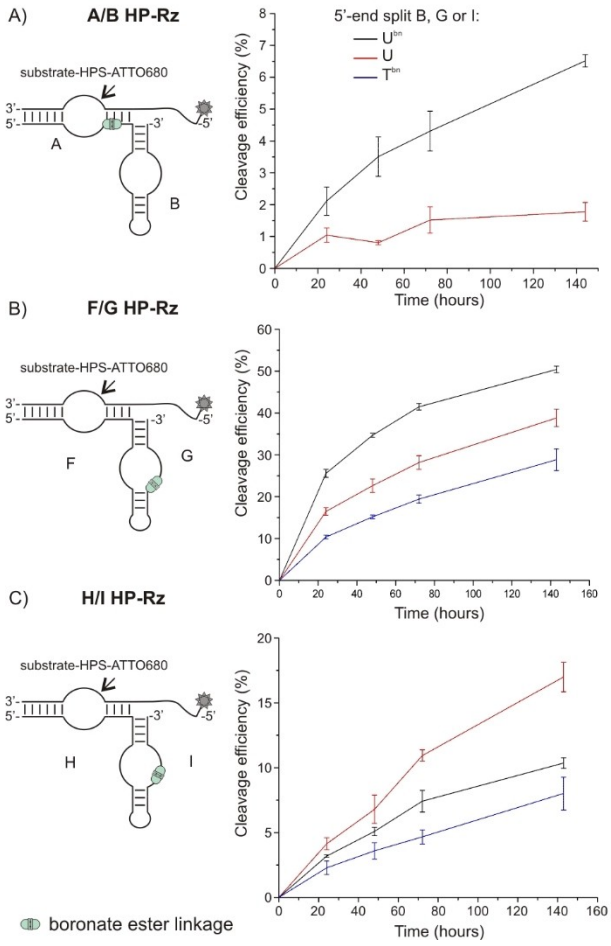

Figure 4. Time course of cleavage reactions of **A)** split ribozyme variants **A/B**, **B)** split ribozyme variants **F/G** and **C)** split ribozyme variants **H/I**. Average data was collected from three independent measurements.

carrying **T^{Bn}** was less suited, activity of **F/G^{TBn}** was even lower than observed for the unmodified split variant. Interestingly, variant **H/I** showed best activity when unmodified fragments were used (17% conversion after 144 h). Neither **U^{Bn}** nor **T^{Bn}** at the 5′-end of fragment I were able to restore cleavage (Figure 4C, Table S5), which implies that the boronate ester, if formed, or alternatively the 5′-terminal boronic acid of one fragment at this position between A^{38} and U^{39} has a distortive effect, eventually interfering with proper folding of the ribozyme.

Cleavage activity in the presence of Catechol

To clearly show the importance of the boronate ester formation for recovery of ribozyme activity, we chose one of the systems to perform competition experiments in the presence of 1000 equivalents of catechol (Figure S21). Catechol as 1,2-*cis*-diol forms a stable ester with boronic acid[15,32] and thus would compete with the 3′-terminal diol of the RNA fragments in our ribozyme assays (Figure 5A).

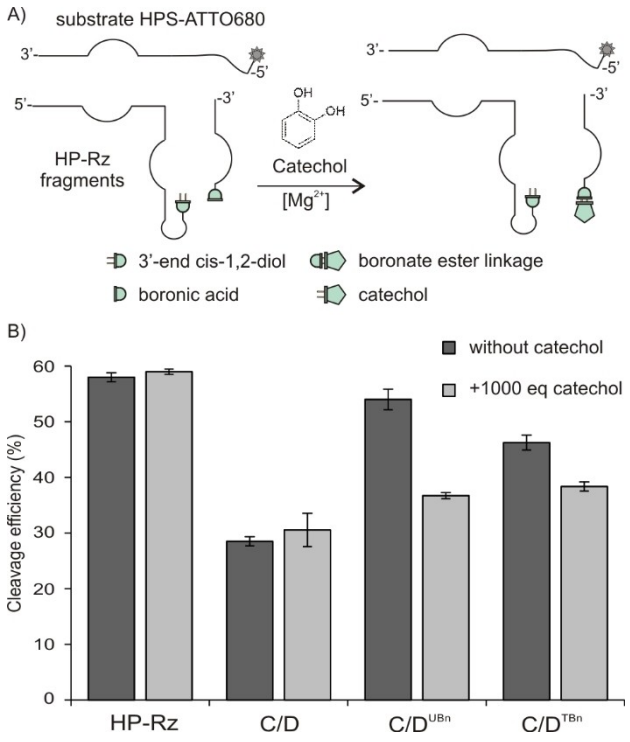

Figure 5. A) Competition experiments with catechol. **B)** Cleavage yields of ribozyme variants are given after three hours reaction at 25 °C, 20 mM $MgCl_2$ and pH 7.5. Equivalents of catechol are in relation to ribozyme fragment D. Average data were collected from three independent measurements.

As we had expected, the presence of catechol virtually did not affect the activity of the parent ribozyme **HP-Rz**, and also not of the unmodified split variant **C/D** (Figure 5B). However, a clear reduction of the cleavage yield was observed, when catechol was added to the cleavage reactions of borono-modified variants **C/D^{UBn}** and **C/D^{TBn}** (Figure 5B). After three hours of reaction, the cleavage yield of variant **C/D^{UBn}** decreased from 54% to 37% (with 1000 equiv. of catechol), nearly matching the activity of the non-modified split variant **C/D**. A similar result was obtained for **C/D^{TBn}**, also here activity decreased to 38% in the presence of 1000 equiv. of catechol (Figure 5B). Further excess of catechol did not lead to further reduction of cleavage.

Ligation reactions

While hairpin ribozyme catalyzed cleavage is less demanding and can proceed also from transiently docked ribozymes, ligation is more dependent on proper folding, requiring a kinetically stable tertiary structure.[33] Therefore, we now have used a three-way junction hairpin ribozyme (Figure S22), which is structurally more stable and thus better suited to support RNA ligation.[25,34] The designed split three-way junction ribozyme variants indeed showed ligation activity (Figure S22). However, we did not observe a supportive effect of boronate ester formation. The borono-modified split variant showed even somewhat lower ligation activity (23% ligation after 3 h, versus 32% for the nonmodified split variant, Figure S22).

Split Aptamer Mango

Encouraged by the results obtained with the hairpin ribozyme, we extended our study to split aptamers and chose the light-up aptamer Mango for split design. Mango has resulted from in vitro selection and binds the biotinylated thiazole orange derivative TO1-B with ~1 nM affinity, thereby enhancing its fluorescence by >1500-fold.[17] Functionality of Mango was virtually lost when splitting the aptamer in two halves (Figure 6, **M/N**) but could be almost fully restored by formation of a boronate ester connecting the two fragments (Figure 6, **M/N^{CNaphtBn}**, orange bar). The split site between G16 and C17 was chosen arbitrarily within the loop of the stem-loop secondary structure, born of the intention of assembling the aptamer from two fragments of virtually equal length. Phenyl- and Naphtyl boronic acid modifications were chosen in the hope that the aromatic systems of both compounds would favor stacking interactions with the nucleobases and thus facilitate folding and boronate ester formation. Both moieties were introduced to Split Mango by either replacing C17 at the 5′-end of fragment **N** (named **N^{PhBn}** or **N^{NaphtBn}**) or being additionally attached to C17 at the 5′-end of that fragment (named **N^{CPhBn}** or **N^{CNaphtBn}**). Thereby, the four modified systems depicted in

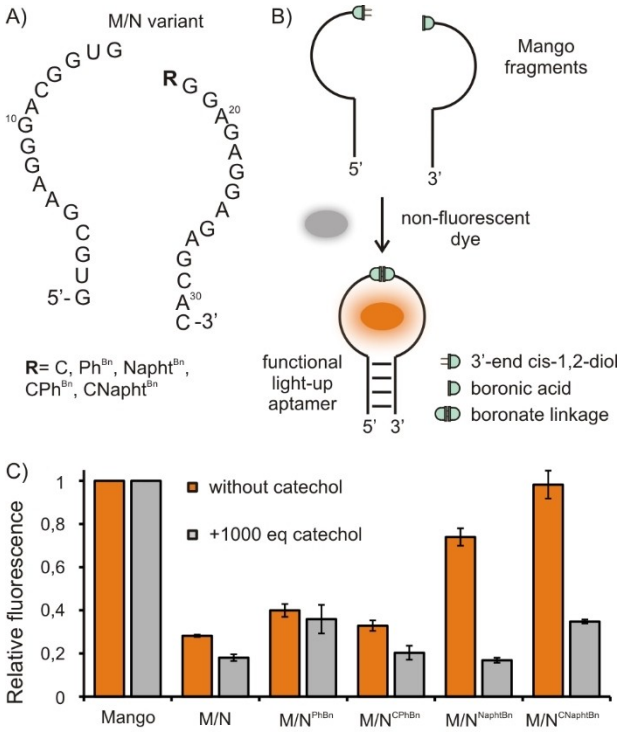

Figure 6. Split Mango aptamer. **A)** Secondary structure of Mango with split site between fragments M and N indicated; **B)** Fluorescence assay for functional characterization of split Mango aptamers; **C)** Fluorescence data. FL = full length aptamer. dark grey bars - no catechol; light grey bars - 1000-fold excess of catechol over RNA splits.

Figure 6 were generated and tested. Whereas the phenylboronic acid modified fragments showed only a slight increase of the aptamer's functionality (Figure 6C, **M/N^{PhBn}** and **M/N^{CPhBn}**, orange bars), the naphthylboronic acid modified fragments were found to almost fully restore it (**M/N^{NaphtBn}** and **M/N^{CNaphtBn}**, orange bars). To further confirm the importance of the boronate ester formation, experiments were repeated in the presence of a 1000-fold excess of catechol, as described above for the hairpin ribozyme studies. A fluorescence decrease was observed, and again, the effect is much stronger for the naphthylboronic acid modified fragments (Figure 6C, light grey bars).

Discussion

Over the past decade, split aptamers and ribozymes made of two or more short nucleic acid strands that assemble to form a functional structure, have emerged as potential tools in diagnostic and therapy.[8] Nevertheless, their application is still rather limited, as the development of a powerful split system is still a challenging task. One important issue is the reduced stability of the split aptamer/ribozyme in comparison to its full length counterpart. Stabilization of the split system can be achieved by structural manipulation, i.e. extension of the individual fragments by additional nucleotides that by complementary base pairing would assist assembly and increase stability of the split aptamer/ribozyme complex.

Alternatively, the fragments of the split system can be decorated with reactive groups, such that the individual strands upon assembly and folding would become covalently linked. In the present study we have used split systems composed of fragments functionalized with a 5′-boronic acid moiety to react with the 3′-terminal *cis*-diol of another fragment, thus forming a boronate ester as covalent internucleosidic linkage. In this way, split ribozymes and aptamers were assembled from two fragments, and formation of functional entities was followed by activity tests, namely cleavage and/or ligation of suitable substrates, or in case of the Mango aptamer fluorescence studies. The boronate ester linkage clearly played an important role in the stabilization of the re-formed functional nucleic acid systems. Competition experiments with addition of catechol confirmed the significance of the linkage for the catalytic activity of split-ribozymes and the functionality of the Mango aptamer. In contrast to the split DNAzymes described recently,[15] the hairpin ribozyme was clearly more sensitive to the replacement of the natural phosphodiester linkage with a boronate ester, probably owing to the functional role that some of the 2′-OH functionalities play. Thus, results obtained with the 5′-boronic acid modified fragments have also allowed us drawing new conclusion and/or confirming previous results on the functional importance of specific 2′-OH groups in the hairpin ribozyme structure. If the split site was positioned in the substrate binding domain between G^{11} and U^{12} of the ribozyme (**A/B** variant, Figures 4A, S18), the ribozyme was not able to efficiently cleave the substrate. The unmodified variant was unstable, could not bind the substrate and not form the catalytic structure. Also, the borono-modified analog **A/B^{UBn}** did not restore activity, which most likely is a result of eliminating hydrogen bonds formed by the 2′-hydroxyl group of G^{11}, essential for formation of a ribose zipper that stabilizes the catalytically active conformation.[35] Much better results were obtained with variant **C/D**, where activity was found even with non-modified fragments, but was clearly higher with the borono-modified variants **C/D^{UBn}** and **C/D^{TBn}** (Table 1). Interestingly, activity was even found for split ribozymes with the boronate ester linkage being placed in the loop area. The stability of loop B is known to be an important parameter for the catalytic activity of the ribozyme. Two fragmentation positions, between G^{36}/U^{37} (**F/G** variant, Figures 4B, S19) and A^{38}/U^{39} (**H/I** variant, Figures 4C, S20) were tested, and both variants, exhibited catalytic activity, which was higher when the fragment modified with **U^{Bn}** was used, as compared to the non-modified one in the **F/G**-variant, but not in the **H/I** variant (Figures 4B, C). The lost activity of the **H/I^{UBn}** variant is possibly owing to a lost contact of the 2′-OH group of A^{38}, which is blocked by formation of the boronate ester. The 2′-OH group of A^{38} forms a hydrogen bond with the nitrogen N7 of G^{+1} involved in the stabilization of the G-binding pocket.[35] Likewise, the substitution of U^{37} and U^{39} with **T^{Bn}** in loop B decreased activity of variants **F/G^{TBn}** and **H/I^{TBn}** even below the level of the non-modified split variants **F/G** and **H/I** (Figures 4B, C), confirming that the 2′-hydroxyl groups of U^{37} and U^{39} also play a role in the stabilization of the G-binding pocket.

While cleavage activity of some variants could be restored by formation of a stabilizing boronate ester linkage, ligation by split hairpin ribozymes proved to be more challenging. The designed split hairpin ribozyme variants were ligation active, however, activity of the borono-modified variant was lower than activity of the non-modified split variant. Ligation is particularly dependent on a properly folded ribozyme with a kinetically stable tertiary structure. Hence, the expected stabilizing effect of the boronate ester may be counteracted by even a slight distortion of the catalytic structure brought about by the non-natural linkage.

For the Mango aptamer, fragments with 5′-terminal **Napht^{Bn}** showed best results of boronate ester formation with the 3′-terminal *cis*-diol of the other fragment and reconstruction of a functional aptamer. This may be a result of the high stacking potential of the large naphtyl aromatic system, bringing in a stabilizing effect to the structure by interacting with the typical quadruplex motif of Mango.[36,37]

Conclusion

We have demonstrated that activity of split hairpin ribozymes as well as functionality of a split Mango aptamer can be controlled through the use of two fragments, one of which being modified with a boronic acid at the 5′-end and the other with a *cis*-diol at the 3′-end. Fragment assembly orients the two moieties in close proximity, such that an internucleoside boronate ester linkage is formed. This results in stabilization of the ribozyme or aptamer structure and restores functionality.

For all the modified split hairpin ribozyme variants, 5′-boronouridine modified fragments performed best among the tested boronic acid derivatives. Nevertheless, in some cases, also Phenyl- or Naphtyl boronic acid derivatives can be good alternatives, as shown for the Mango aptamer. Split versions of light-up aptamers have great potential for intracellular monitoring, imaging and sensing of biomolecules, but often suffer from insufficient stability.[8] The linkage of assembled aptamer fragments by a boronate ester as shown herein, can overcome this limitation and thus improve aptamer design and application for numerous purposes, i.e. general nucleic acid probing,[27] cellular small nc-RNA imaging,[38] or aptamer-based proximity labeling.[39]

Apart from the potential of such split architectures for the development of novel biosensors, our results are also relevant in the context of the RNA world hypothesis.[40] A still unsolved question is how the first rather large RNAs that would be required for fulfilling complex functions may have emerged. An attractive scenario is that shorter sequences may have interacted to form functional assemblies. Since boronate esters are supposed to have appeared on the early Earth,[41] it is reasonable to hypothesize that the formation of internucleosidic boronate ester linkages as demonstrated herein, may have assisted RNA assembly and increased the stability of the assembled structures. It is a particular attractive feature of the boronate ester linkage that its formation is easily reversible in dependence on the environment and thus allows for self-repair and self-adaptation. Moreover, reversible chemistry allowing for chain-forming as well as chain-breaking steps is a major requirement for biological self-organization. The boron chemistry for the controlled reversible assembly of functional nucleic acids as demonstrated herein is perfectly suited to fulfill this requirement and thus potentially may have played an important role in early life on earth.

Experimental Section

Phosphitylation of borono-modified derivatives: For conversion to phosphoramidites, 4-hydroxyphenyl boronic acid (Merck) and naphtylboronic acid (BioNet) protected as pinacol ester, and the 5′-boronic acid derivatives of uridine and thymidine synthesized previously with a MIDA protection group[12,29] were used. All flasks and reagents were treated to avoid the presence of moisture and the reaction took place under argon atmosphere. The educts were co-evaporated three times with dry dichloromethane or acetonitrile, depending on its solubility, and dissolved in dry dichloromethane (0.1 M for nucleobase derivatives and 0.3 M for phenyl- or naphtylboronic acid). Dry diisopropylethylamine (1.8 equiv.) and 2-cyanoethyl-*N,N*-diisoprpopylchloro-phosphoramidite (1.5 equiv.) were slowly added and the solutions were stirred at room temperature. Without further work-up the crude products were directly purified with a small and quick silica gel column chromatography.

Chemical synthesis of oligonucleotides: All modified and unmodified oligoribonucleotides were synthesized by standard solid phase phosphoramidite chemistry at 1 μmol scale using a Pharmacia Gene Assembler Plus. Benzylmercaptotatrazol (BMT, emp Biotech) was used as activator. The prepared phosphoramidites were solved in dry acetonitrile (0.12 M for nucleoside derivatives and 0.15 M for the phenyl- or naphtylboronic acid). The solutions of phosphoramidites, BMT, and acetonitrile were kept over molecular sieve (0.3 nm, Roth). The coupling time for all phosphoramidites was 5 min. All unmodified oligonucleotides were synthesized "trityl-off." The obtained modified and unmodified RNAs (Table S3 and S4) were cleaved from the support and deprotected using NH_3 (30%) in a 1:1 mixture with 8 M ethanolic amine, followed by treatment with TEAx3HF. Deprotected crude RNAs were purified by gel electrophoresis using 15% denaturing polyacrylamide gels. Elution of the main product was performed using a 0.3 M NaOAc (pH 5.0) followed by EtOH precipitation.

Cleavage assays: The full-length ribozyme HP-Rz or its split versions (2 μM), and the substrate HPS-ATTO680 (20 nM), were incubated in Tris HCl buffer (50 mM, pH 7.5 or 8.7), for 2 min at 90 °C followed by 15 min at 25 °C. For the competition studies, catechol (1000 equivalent over the ribozyme) was also added for the pre-incubation step. The cleavage reaction was started by addition of $MgCl_2$ (20 mM) and left to proceed at 25 °C. At individual times, 0.5 μL of sample were taken out of the reaction mixture and immediately added to 9.5 μL of stop mix (7 M urea, 50 mM EDTA, and 0.05% blue dextran). Samples were analyzed by electrophoresis through 10% denaturing polyacrylamide gels using the LI–COR DNA sequencer 4200bw (1500 V, 45 °C, 0.6x TBE, 700 nm). The software Image Studio Lite Version 5.2 was used for the quantification of cleaved and uncleaved substrate signals. The collected data were fitted with nonlinear exponential $y = a(1-e^{-bx})$ equation to obtain the kinetic parameters k_{obs} (corresponding to b) and max. percentage of cleavage (corresponding to a).

Fluorescence assay with the Mango aptamer: Reaction conditions were adapted to Dolgosheina et al.[16] Briefly, full-lengths or split versions of the Mango aptamer (10 μM) were incubated in buffer (10 mM Na_3PO_4, 140 mM KCL, 1 mM $MgCl_2$, pH 7.2) for 2 min at 95 °C, followed by addition of Thiazole Orange biotin (TO1-B) in equimolar amounts. The mixture was then put on ice for 25 min. Fluorescence was measured on a TECAN Infinite 200 pro at $\lambda_{em} = 535$ (±20) nm, excitation wavelength was $\lambda_{ex} = 505$ (±9) nm.

Acknowledgements

The Agence Nationale de la Recherche and the Deutsche Forschungsgemeinschaft are gratefully acknowledged for financial support (ANR PCRI "TEMPLAR"-16-CE92-0010-01; DFG MU1396/19). Open Access funding enabled and organized by Projekt DEAL.

Conflict of Interests

The authors declare no conflict of interest.

Data Availability Statement

The data that support the findings of this study are available from the corresponding author upon reasonable request.

Keywords: aptamer · boronate linkage · ribozyme · RNA · split structure

[1] A. V. Dass, S. Wunnava, J. Langlais, B. von der Esch, M. Krusche, L. Ufer, N. Chrisam, R. C. A. Dubini, F. Gartner, S. Angerpointner, C. F. Dirscherl, P. Rovó, C. B. Mast, J. Šponer, C. Ochsenfeld, E. Frey, D. Braun, *ChemSysChem.* **2023**, *5*, e20220002 .
[2] K. Kruger, P. J. Grabowski, A. J. Zaug, J. Sands, D. E. Gottschling, T. R. Cech, *Cell* **1982**, *31*, 147.
[3] M. P. Robertson, G. F. Joyce, *Cold Spring Harbor Perspect. Biol.* **2012**, *4*, a003608.
[4] Z.-Y. J. Zhan, D. G. Lynn, *J. Am. Chem. Soc.* **1997**, *119*, 12420–12421.
[5] A. E. Engelhart, B. J. Cafferty, C. D. Okafor, M. C. Chen, L. D. Williams, D. G. Lynn, N. V. Hud, *ChemBioChem* **2012**, *13*, 1121.
[6] Y. Liu, M. C. A. Stuart, M. D. Witte, E. Buhler, A. K. H. Hirsch, *Chem. Eur. J.* **2017**, *23*, 16162.
[7] N. Roy, B. Bruchmann, J.-M. Lehn, *Chem. Soc. Rev.* **2015**, *44*, 3786.
[8] M. Debiais, A. Lelievre, M. Smietana, S. Müller, *Nucleic Acids Res.* **2020**, *48*, 3400.
[9] G. A. Ellis, M. J. Palte, R. T. Raines, *J. Am. Chem. Soc.* **2012**, *134*, 3631.
[10] L. Li, Z. Bai, P. A. Levkin, *Biomaterials* **2013**, *34*, 8504.
[11] A. R. Martin, I. Barvik, D. Luvino, M. Smietana, J.-J. Vasseur, *Angew. Chem. Int. Ed.* **2011**, *50*, 4193.
[12] A. G. Molina, I. Barvik, S. Müller, J.-J. Vasseur, M. Smietana, *Org. Biomol. Chem.* **2018**, *16*, 8824.
[13] M. Debiais, J.-J. Vasseur, S. Müller, M. Smietana, *Synthesis* **2020**, *52*, 2962.
[14] M. Debiais, J. J. Vasseur, M. Smietana, *Chem. Rec.* **2022**, e202200085.
[15] M. Debiais, A. Lelievre, J.-J. Vasseur, S. Müller, M. Smietana, *Chem. Eur. J.* **2021**, *27*, 1138.
[16] S. W. Santoro, G. F. Joyce, *PNAS* **1997**, *94*, 4262.
[17] E. V. Dolgosheina, S. C. Y. Jeng, S. S. S. Panchapakesan, R. Cojocaru, P. S. K. Chen, P. D. Wilson, N. Hawkins, P. A. Wiggins, P. J. Unrau, *ACS Chem. Biol.* **2014**, *9*, 2412.
[18] C. L. Peebles, P. S. Perlman, K. L. Mecklenburg, M. L. Petrillo, J. H. Tabor, K. A. Jarrell, H.-L. Cheng, *Cell* **1986**, *44*, 213.
[19] A. Hampel, R. Tritz, *Biochemistry* **1989**, *28*, 4929.
[20] N. G. Walter, K. J. Hampel, K. M. Brown, J. M. Burke, *EMBO J.* **1998**, *17*, 2378.
[21] S. Müller, B. Appel, T. Krellenberg, S. Petkovic, *IUBMB Life* **2012**, *64*, 36.
[22] R. Hieronymus, S. Müller, *Ann. N. Y. Acad. Sci.* **2019**, *1447*, 135.
[23] S. Müller, *Ann. N. Y. Acad. Sci.* **2015**, *1341*, 54.
[24] R. Hieronymus, S. Müller, *ChemSystemsChem* **2021**, *3*, e2100003.
[25] B. M. Chowrira, A. Berzal-Herranz, C. F. Keller, J. M. Burke, *J. Biol. Chem.* **1993**, *268*, 19458.
[26] R. Welz, C. Schmidt, S. Müller, *Biochem. Biophys. Res. Commun.* **2001**, *283*, 648.
[27] Y. V. Gerasimova, D. D. Nedorezova, D. M. Kolpashchikov, *Methods* **2022**, *197*, 82.
[28] C. Shin, J. N. Choi, S. I. Song, J. T. Song, J. H. Ahn, J. S. Lee, Y. D. Choi, *Nucleic Acids Res.* **1996**, *24*, 2685.
[29] A. Berzal-Herranz, S. Joseph, B. M. Chowrira, S. E. Butcher, J. M. Burke, *EMBO J.* **1993**, *12*, 2567.
[30] D. Luvino, C. Baraguey, M. Smietana, J.-J. Vasseur, *Chem. Commun.* **2008**, 2352.
[31] A. R. Martin, J.-J. Vasseur, M. Smietana, *Chem. Soc. Rev.* **2013**, *42*, 5684.
[32] F. Coumes, A. Malfait, M. Bria, J. Lyskawa, P. Woisel, D. Fournier, *Polym. Chem.* **2016**, *7*, 4682.
[33] S. Gaur, J. E. Heckman, J. M. Burke, *RNA* **2008**, *14*, 55.
[34] Z. Y. Zhao, T. J. Wilson, K. Maxwell, D. M. Lilley, *RNA* **2000**, *6*, 1833.
[35] P. B. Rupert, A. R. Ferré-D'Amaré, *Nature* **2001**, *410*, 780.
[36] R. J. Trachman, N. A. Demeshkina, M. W. L. Lau, S. S. S. Panchapakesan, S. C. Y. Jeng, P. J. Unrau, A. R. Ferré-D'Amaré, *Nat. Chem. Biol.* **2017**, *13*, 807.
[37] R. J. Trachman, A. Abdolahzadeh, A. Andreoni, R. Cojocaru, J. R. Knutson, M. Ryckelynck, P. J. Unrau, A. R. Ferré-D'Amaré, *Biochemistry* **2018**, *57*, 3544.
[38] A. Autour, S. C. Y. Jeng, A. D. Cawte, A. Abdolahzadeh, A. Galli, S. S. S. Panchapakesan, D. Rueda, M. Ryckelynck, P. J. Unrau, *Nat. Commun.* **2018**, *9*, 656.
[39] D. Englert, R. Matveeva, M. Sunbul, R. Wombacher, A. Jäschke, *Chem. Commun.* **2021**, *57*, 3480.
[40] K. LeVay, H. Mutschler, *Emerg. Top. Life Sci.* **2019**, *3*, 469.
[41] R. Scorei, *Origins Life Evol. Biospheres* **2012**, *42*, 3.

Manuscript received: January 23, 2023
Accepted manuscript online: March 31, 2023
Version of record online: May 5, 2023